Registering Cortical Surfaces Based on Whole-Brain Structural Connectivity and Continuous Connectivity Analysis

Boris Gutman, Cassandra Leonardo, Neda Jahanshad, Derrek Hibar, Kristian Eschenburg, Talia Nir, Julio Villalon, and Paul Thompson

Imaging Genetics Center, INI, University of Southern California, USA

Abstract. We present a framework for registering cortical surfaces based on tractography-informed structural connectivity. We define connectivity as a continuous kernel on the product space of the cortex, and develop a method for estimating this kernel from tractography fiber models. Next, we formulate the kernel registration problem, and present a means to non-linearly register two brains' continuous connectivity profiles. We apply theoretical results from operator theory to develop an algorithm for decomposing the connectome into its shared and individual components. Lastly, we extend two discrete connectivity measures to the continuous case, and apply our framework to 98 Alzheimer's patients and controls. Our measures show significant differences between the two groups.

Keywords: Diffusion MRI, Cortical Surface Registration, Connectivity Analysis, Data Fusion.

1 Introduction

With the advent of diffusion MRI, and the wealth of information contained within this modality, the subject of fusing structural connectivity information with anatomical knowledge has seen tremendous development. This fusion is straightforward if we restrict our diffusion analysis to summary voxel-wise measures such as Fractional Anisotropy (FA) or Mean Diffusivity. The problem becomes more difficult when we examine the connectivity information provided by tractography fiber models. Because fibers sets are not topologically equivalent across individual brains the usual solutions for image registration and segmentation problems cannot be trivially extended to these objects. Thus, it is not obvious how to fuse them with anatomical image processing in a straight-forward manner.

Several approaches have been proposed for fusing structural connectivity with anatomy. Perhaps the most common of these relies on the concept of a connectivity matrix or a graph between anatomically defined regions of interest (ROI). The strength of a connection between each region pair is estimated by counting the number of fiber models between the two ROI's [1]. The resulting graph can be analyzed using the standard graph theory measures [2], which can reveal interesting global and region-specific features of the brain's connectome, such as its "small-worldness," or the degree to which the network is compartmentalized into sub-networks [2].

P. Golland et al. (Eds.): MICCAI 2014, Part III, LNCS 8675, pp. 161–168, 2014.

Alternatively, the DICCCOLs approach [3] seeks to identify small seed regions within the cortex which contain fibers with a similar geometric signature. The idea is that a geometric signature of the connection paths points to similar functional role across brains. Another exciting approach clusters brain regions spectrally with only the tractography seed regions as an anatomical prior [4].

Fiber- and anatomy-based registration fusion has also seen some development both with surface and volumetric anatomy models. Siless et al. [5] developed a framework based on geometric currents to drive inter-fiber set registration in combination with T1-weighted MRI image registration. Alternatively, Petrovic [6] assumed cortical alignment and registered thalamic surfaces based on the cortical fiber projections. In all of these cases, the full fiber geometry plays an integral part in driving the correspondence search, or some part of the brain is assumed to be perfectly aligned. The same is true for the region identification technique of DICCOLS: structural connectivity equivalence is estimated indirectly with a brief summary measure, defined as a histogram of orientations along the fiber. Unlike previous registration fusion approaches, we choose to apply the connectivity information supplied by the fiber model directly in a continuous registration setting, which significantly complicates the problem. Our goal is to find a correspondence between brains so that the corresponding regions are similarly connected. As in [1], we treat fiber geometry as a secondary feature, useful only in identifying the implied connection between brain regions. In this approach, two fibers with different geometry connecting the same pair of cortical locations are deemed equivalent.

Extending the discrete connectivity modeling of [2] to the continuous setting, we consider the connectome as a continuous kernel on the product space of the brain with itself. This is a natural extension of the graph representation for the discrete case. We treat each fiber as an instance of a connection on this space, with some possible geometric error. This idea naturally leads to kernel density estimation on the connectome space based on the set of fibers. Next, we would like to find a smooth non-linear invertible spatial warp that minimizes the difference between two brains' connectomes. Direct optimization of this problem poses a significant computational challenge. Instead, we decompose the kernel into its corresponding eigenfunctions, here called "eigen-networks," and use Mercer's Theorem for kernel matching and reconstruction. This convenient decomposition allows us to estimate the shared and subject-specific components of the connectome prior to registration, while the minimization problem is reduced to the usual multi-channel registration on the original domain of the cortex. We restrict our search to cortico-cortical and cortico-thalamic connections, which allows us to use the white matter boundary surface of the cortex to compactly represent the domain of the brain. Finally, we propose two continuous graph theory measures based on their discrete equivalents, and compute group differences between 48 Alzheimer's patients and 50 control participants from the ADNI cohort.

2 Continuous Connectome Estimation

We define the continuous connectome as a symmetric non-negative real-valued function $K: \mathcal{C} = \Omega \times \Omega \to \mathbb{R}^+ \ by \ (x, y) \mapsto K(x, y)$ from the product space of the cortical domain to the non-negative real numbers. $K(x, y)$ represents the strength of the

connection between the points x and y in the brain. As we are dealing with cortical surface models, our cortical domain is itself a mapping from the two-sphere into space: $\Omega = \mathcal{M}: \mathbb{S}^2 \to \mathbb{R}^3$. Since we perform our registration parametrically on $\mathbb{S}^2$, and because our $\mathcal{M}$ is diffeomorphic and area-preserving [7], we may equivalently set $\Omega = \mathbb{S}^2$ for convenience. While we do not have sufficiently resolved data to compute the true fiber-based connectivity, except using the coarsest resolution, we can apply the standard kernel density estimation. In this approach, we treat each fiber model as a representation of potentially many true fibers, with some possible error in its placement in the space $\mathcal{C}$. Given N_{fibers} fiber models, we project the two ends of each model onto the gray-white matter boundary, resulting in sets of point pairs $\{p_1^i, p_2^i\}$, discounting fibers that do not have both ends sufficiently close to the boundary. We apply the product of two Gaussian kernels on $\mathbb{S}^2$, [8] $G_\sigma: \mathbb{S}^2 \times \mathbb{S}^2 \to \mathbb{R}^+$, resulting in our non-local connectome estimation:

$$K_{non-local}(x,y) = \sum_{1=i\le N_{fibers}} G_\sigma(x, p_1^i)\, G_\sigma(p_2^i, y). \tag{1}$$

The parameter σ is set empirically so that the spherical area within the half-maximum of G_σ is equal to $\frac{2\pi}{N_{fibers}}$.

An aspect of brain connectivity which does not arise in the discrete approach is the modelling of local connections. Because tractography fiber models do not capture local connections at our cortical mesh resolution, we estimate local connectivity based on cortical geometry alone. We set local connectivity as

$$K_{local}(x,y) = G_\sigma(x,y). \tag{2}$$

A brief literature search [9] suggests we a golden ratio of local to global connectivity at $R_g = 1/3$. Thus, we set the complete connectivity kernel as

$$K = \frac{1}{N_{fibers}}\left(K_{non-local} + R_g K_{local}\frac{\|K_{non-local}\|}{\|K_{local}\|}\right), \tag{3}$$

where $\|K\| = \left(\iint_{\mathcal{C}} K(x,y)^2 dxdy\right)^{1/2}$.

3 Kernel Registration

Given two connectomes $K_1(x,y)$, $K_2(x,y)$, we assume that K_1 and K_2 differ from their mutual connectivity profile by a scale s, a smooth invertible warp $f: \Omega \to \Omega$ and an additive *individual* component:

$$K_{12,\ mutual}(x,y) = s_i\left[K_i\left(f_i[x], f_i[y]\right) - K_{i,\ indiv}(f_i[x], f_i[y])\right]. \tag{4}$$

For convenience, we set $f_1 = Id$. The kernel norm defined in the previous section suggests a cost function analogous to the L^2 fidelity in image registration:

$$C(K_1, K_2, f) = \iint_{\mathcal{C}} [K_1(x,y) - K_2(f[x], f[y])]^2 \, dxdy \tag{5}$$

There are two issues with this formulation. First, while we have scaled the *full* kernels identically, we cannot know that their *mutual* connectomes will have the same scale. Second, a direct optimization of (5) is computationally expensive, as every point update requires full domain integration. Instead, we would like to estimate the mutual and individual components of the kernels prior to registration, while decoupling the two instances of $f[x]$ in (5). To this end, we decompose the kernels into the eigenfunctions, or "eigen-networks," of their linear operators, $Ae_i = \lambda_i e_i$, where $Af[y] = \int_\Omega K(x,y) f(x) dx$. According to Mercer's Theorem [10], we can reconstruct a symmetric positive definite (SPD) kernel by $K(x,y) = \sum_i \lambda_i e_i(x) e_i(y)$. This well-known result from operator theory provides an unexpected utility towards solving the kernel registration problem. To use it, we must only satisfy the SPD condition, which can be done by setting $K(x,x) = \int_\Omega K(x,y) dy$.

Since we assume that $K_{12,\ mutual}$ is itself SPD, we can make the assumption in (4) slightly stronger, asserting that the eigen-networks of $K_{12,\ mutual}$ and $K_{i,\ indiv}$ are orthogonal. On the other hand, because our non-linear correspondence search is local, we assume that some spatial overlap between the corresponding eigen-networks of $K_{12,\ mutual}$ and those of K_1 and K_2 must already exist. Note that a similar assumption is prevalent in standard non-linear registration algorithms. This allows us to estimate the mutual connectome by projecting the eigen-networks of the target connectome onto the corresponding invariant subspaces of the moving template connectome. We estimate the likelihood that for some small f, the transformed network of A_1, $f * e_i^1$, belongs to A_2 by

$$P[\{f * e_i^1\} \epsilon\ spectrum(A_2)] = \frac{\langle A_2 e_i^1, e_i^1 \rangle}{\left\| A_2 e_i^1 \right\|^2}, \tag{6}$$

where $\langle g, h \rangle = \int_\Omega gh$. For networks passing a threshold, we estimate their eigenvalue for A_2 as $\omega = \frac{\langle A_2 e_i^1, A_2 e_i^1 \rangle}{\langle A_2 e_i^1,\ e_i^1 \rangle}$, and project e_i^1 onto the invariant subspace of A_2 defined by ω. Via this process, we identify the set of mutual eigen-networks of the target and the moving template connectomes, $\boldsymbol{E_M} = \{e_{i_k}^1, e_{j_k}^2, w_k\}$.

A major difference between spectral decomposition of matrices and infinite-dimensional operators relates to eigenvalue multiplicity. In particular, it is possible to have non-isolated eigenvalues, and infinite-dimensional invariant subspaces. However, because our operator kernels are finites sum of weighted basis functions, we can say that the operators are finite-rank, and therefore necessarily compact [10]. This fact has a nice practical implication: the multiplicity of the eigenvalues is at most countable with the only possible limit point at 0. This means that any neighborhood $N_\epsilon(\omega), \omega > \epsilon$, contains a finite number of eigenvalues counting multiplicity, which makes step 1 in the following search feasible even in the true continuous case:

Algorithm 1 (mutual connectome estimation)
Given SPD kernels K_1, K_2, their corresponding operators A_1, A_2 and the ordered spectral decompositions $\{e_i^1, \lambda_i^1\}$, $\{e_j^2, \lambda_j^2\}$, set mutual networks $\boldsymbol{E_M} = \{e_{i_k}^1, e_{j_k}^2, w_k\} = NULL$. k = 1

For i=1:N
Compute $P = \frac{\langle A_2 e_i^1, e_i^1 \rangle}{\|A_2 e_i^1\|^2}$ (6)
  if(P > P_tol)
    1. Set $\omega = \frac{\|A_2 e_i^1\|^2}{\langle A_2 e_i^1, e_i^1 \rangle}$, set $\boldsymbol{E_i} = \left\{ e_j^2 \middle| 2\frac{|\lambda_j^2 - \omega|}{\lambda_j^2 + \omega} < \epsilon \right\}$
Project e_i^1 onto $span\{\boldsymbol{E_i}\}$, $e_{proj} = Proj_{span\{\boldsymbol{E_i}\}} e_i^1$
    if($\|e_{proj}\|$ > proj_tol)
      3. $e_{proj} \rightarrow e_{proj}/\|e_{proj}\|$
      4. $n = \max_j \{\langle e_{proj}, e_j^2 \rangle \mid e_j^2 \in \boldsymbol{E_i}\}$, set $e_n^2 = e_{proj}$
      5. Re-orthonormalize $\boldsymbol{E_i}$, starting with e_n^2
      6. Estimate new eigenvalues $\lambda_j^2 = \|A_2 e_j^2\|$, $e_j^2 \in \boldsymbol{E_i}$
      7. $w_k = \sqrt{\lambda_n^2 \lambda_i^1}$, $i_k = i$, $j_k = n$.
      8. Insert $(e_{i_k}^1, e_{j_k}^2, w_k)$ into $\boldsymbol{E_M}$, k = k + 1
    endif
  endif
end
Return $\boldsymbol{E_M}$

The mutual connectome can now be estimated as $K_{12,\ mutual}(x, y) = \sum_{e_i^1 \in \boldsymbol{E_M}} \lambda_i^1 e_i^1(x) e_i^1(y) e_i^1$. Finally, we define the mutual connectome mismatch cost:

$$\mathrm{C}(\boldsymbol{E_M}, f) = \int_\Omega \sum_{\left(e_{i_k}^1, e_{j_k}^2, w_k\right) \in \boldsymbol{E_M}} w_k \left| e_{i_k}^1(x) - e_{j_k}^2(f[x]) \right|^2 dx. \quad (7)$$

The solution of this functional is straightforward, and has been described elsewhere. It is worth noting that the gradient direction (7) is invariant to kernel scale, as it is based on normalized eigen-networks. As our parametric domain is $\mathbb{S}^2$, we use a recent spherical fluid registration algorithm [7], incorporating mean and Gaussian curvature mismatch in addition to (7). In this way we combine anatomical and connectivity information, registering brain connectivity structure directly across subjects.

4 Continuous Connectomics

Use of graph theory in brain connectivity studies has exploded in recent years; to this end, we contribute two weighted continuous analogues of the nodal degree and clustering coefficient measures [2]. Nodal degree, defined for discrete weighted graphs as

$k_d(x) = \sum_{y \in \Omega_d} K_d(x,y)$, where the subscript d means the discrete analogue of previous definitions, is defined here as the *connectedness map*

$$k(x) = \int_\Omega K(x,y)dy = K(x,x). \tag{8}$$

The discrete clustering coefficient is defined as $C_d(x) = \frac{2t_d(x)}{k_{db}(x)(k_{db}(x)-1)}$, where k_{db} is the binarisation of k_d, and $t_d(x) = \sum_{y,z \in \Omega_d} [K_d(x,y)K_d(x,z)K_d(y,z)]^{1/3}$ is the geometric mean of triangles. Our analogue geometric triangle mean is defined as

$$t(x) = \iint_{\mathcal{C}} [K(x,y)K(x,z)K(y,z)]^{1/3}\, dydz, \tag{9}$$

and the analogue of k_{db} is defined as the area of k's support:

$$C(x) = \frac{2t(x)}{\left[\int_{\{y \in \Omega | K(x,y)>0\}} dy\right]^2}. \tag{10}$$

5 Implementation

Our cortical surfaces are extracted with FreeSurfer, and mapped into correspondence on $\mathbb{S}^2$ by registering mean and Gaussian curvatures [7]. Tractography is performed by the Hough transform method [11], with fibers thresholded for length, resulting in 8-10K fibers. About 90% of these pass the threshold for interior ends being sufficiently close to the white matter surface, set at 10 mm. Connectome kernels are projected onto an equiangular spherical grid, with roughly 16.5K vertices per hemisphere, or 33K total. We use the Galerkin method [12] to estimate the eigen-network. The Galerkin method reduces an operator eigenvalue problem to a finite matrix problem, projecting the operator onto a finite set of basis functions. Our basis functions are the step functions defined by the equiangular sampling. We compute up to N eigenvalues, where N is the minimum number needed to approximate the kernel within a tolerance: $tol < \|K - K_N\|/\|K\|$, $K_N(x,y) = \sum_{i<N} \lambda_i e_i(x) e_i(y)$. We ignore the diagonal for this computation, as incorporating it gives optimistic error estimates.

We concede that a continuous formulation on paper often leads to the same implementation as a discrete one. In this case, though, the continuous formalism leads to a basic implementation difference: the area weights of the samples are taken into consideration. This is true both for the eigenvalue problem, which becomes generalized by the area matrix, and for continuous connectivity measures. In the latter case, we can think of the approximate kernel as a large weighted graph, *with weighted nodes*.

6 Experiments

We applied our method to 98 ADNI images. The participants were 48 AD patients and 50 controls. We chose an additional representative control subject to serve as the target. Following anatomical registration, we computed the connectome kernels and

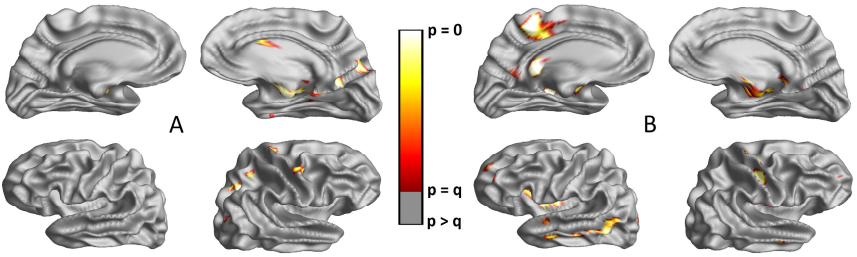

Fig. 1. Corrected p-maps for AD-NC difference in (A) clustering coefficient (10), and (B) connectedness, a.k.a. continuous nodal degree (8). Although it is mostly occluded, the left medial temporal lobe contains the most significant differences.

spectral decompositions of each subject. Each kernel had around 60M non-zero entries, making the connectome roughly 95% sparse. We set the kernel approximation tolerance at 0.1, requiring between 800 and 1200 eigen-networks. Approximately one-third of the target networks were matched to each moving kernel, depending on the participant. This set of networks was then registered to the target's while maintaining low curvature mismatch for anatomically correct correspondence, taking roughly 30 minutes for full combined connectivity registration.

In the first experiment, we computed the change in kernel mismatch, using both full and mutual network sets for kernel approximation. Results are displayed in Table 1, showing improvement in connectome alignment due to connectivity registration. In the second experiment, we performed a mass-univariate t-test over the cortical surface comparing connectedness and clustering coefficient maps between AD and control participants. Both measures passed False Discovery Rate (FDR) correction. FDR threshold for connectedness was $q = 1.0x10^{-3}$ for the right hemisphere, and $q = 1.9x10^{-3}$ for the left. For clustering coefficient, $q = 1.7x10^{-3}$ for the right hemisphere and $q = 2.5x10^{-5}$ for the left. In a related experiment, we made the same comparisons based only on anatomical registration. While the uncorrected p-maps were similar, right hemisphere connectedness and left clustering coefficient did not pass FDR. This suggests improved sensitivity due to the connectome registration. Corrected p-maps of these tests are displayed in Figure 1.

7 Conclusion

We have presented a framework for fusing connectivity information with cortical surface anatomy for a joint analysis. There are four distinct contributions: (1) the definition of a continuous connectome space and a method for estimating continuous kernels from fiber models; (2) an algorithm for defining a mutual connectome shared by two brains; (3) a spatial correspondence search between two connectome kernels, directly registering the brains' structural connectivities; (4) an adaptation of graph theory measures to the continuous setting. The final result is a pipeline for joint cortical surface and connectivity analysis that opens an exciting new way to explore the brain. Future work will ground our connectome estimation more strongly in biological knowledge and connect the eigen-network concept with functional connectivity.

Table 1. Relative difference between target and moving template connectomes before (Col. 1) and after (Col. 2) connectome registration (see section 5). Top row: full connectivity alignment. Bottom row: joint connectivity alignment. (Mean and standard deviation of 98 subjects).

	Anatomy only	Anatomy + connectivity	Individual improvement
Full kernel	0.528 +/-0.101	0.43 +/-0.12	0.098 +/-0.089
Mutual kernel	0.32 +/-0.082	0.12 +/-0.099	0.2 +/-0.089

References

1. Duarte-Carvajalino, J.M., Jahanshad, N., Lenglet, C., McMahon, K.L., de Zubicaray, G.I., Martin, N.G., Wright, M.J., Thompson, P.M., Sapiro, G.: Hierarchical topological network analysis of anatomical human brain connectivity and differences related to sex and kinship. Neuroimage 59, 3784–3804 (2012)
2. Rubinov, M., Sporns, O.: Complex network measures of brain connectivity: Uses and interpretations. Neuroimage 52, 1059–1069 (2010)
3. Zhu, D., Li, K., Guo, L., Jiang, X., Zhang, T., Zhang, D., Chen, H., Deng, F., Faraco, C., Jin, C., Wee, C.Y., Yuan, Y., Lv, P., Yin, Y., Hu, X., Duan, L., Han, J., Wang, L., Shen, D., Miller, L.S., Li, L., Liu, T.: DICCCOL: dense individualized and common connectivity-based cortical landmarks. Cereb Cortex 23, 786–800 (2013)
4. Lecoeur, J., Ingalhalikar, M., Verma, R.: Reproducibility of connectivity based parcellation: primary visual cortex. Proc. Int. Soc. Magn. Reson. Med. Sci. Meet. Exhib. Int. 2089 (2013)
5. Siless, V., Glaunès, J., Guevara, P., Mangin, J.-F., Poupon, C., Le Bihan, D., Thirion, B., Fillard, P.: Joint T1 and brain fiber log-demons registration using currents to model geometry. In: Ayache, N., Delingette, H., Golland, P., Mori, K. (eds.) MICCAI 2012, Part II. LNCS, vol. 7511, pp. 57–65. Springer, Heidelberg (2012)
6. Petrović, A., Smith, S., Menke, R., Jenkinson, M.: Methods for Tractography-Driven Surface Registration of Brain Structures. In: Yang, G.-Z., Hawkes, D., Rueckert, D., Noble, A., Taylor, C. (eds.) MICCAI 2009, Part I. LNCS, vol. 5761, pp. 705–712. Springer, Heidelberg (2009)
7. Gutman, B.A., Madsen, S.K., Toga, A.W., Thompson, P.M.: A Family of Fast Spherical Registration Algorithms for Cortical Shapes. Multimodal Brain Image Analysis (MBIA 2013) (2013)
8. Chung, M.K., Hartley, R., Dalton, K.M., Davidson, R.J.: Encoding Cortical Surface by Spherical Harmonics. Stat. Sinica 18, 1269–1291 (2008)
9. Rubenstein, J.L., Merzenich, M.M.: Model of autism: increased ratio of excitation/inhibition in key neural systems. Genes. Brain Behav. 2, 255–267 (2003)
10. Kreyszig, E.: Introductory functional analysis with applications. Krieger Pub. Co., Malabar (1989)
11. Aganj, I., Lenglet, C., Jahanshad, N., Yacoub, E., Harel, N., Thompson, P.M., Sapiro, G.: A Hough transform global probabilistic approach to multiple-subject diffusion MRI tractography. Medical Image Analysis 15, 414–425 (2011)
12. Beattie, C.: Galerkin Eigenvector Approximations. Math. Comput. 69, 1409–1434 (2000)